Journal of the Brazilian Society of Mechanical Sciences and Engineering (2018) 40:530
https://doi.org/10.1007/s40430-018-1447-3

TECHNICAL PAPER

Thermodynamics by melting in flow of an Oldroyd-B material

T. Hayat[1,2] · Khursheed Muhammad[1] · A. Alsaedi[2] · S. Asghar[3]

Received: 16 April 2018 / Accepted: 8 October 2018 / Published online: 22 October 2018

Abstract

This research reports heat transfer via melting in stagnation point flow of non-Newtonian fluid by a nonlinear stretchable sheet of variable thickness. An incompressible fluid with constant applied uniform magnetic field is inspected. Modeling is based on the constitutive relation of subclass of rate type materials, namely the Oldroyd-B fluid. Heat transfer process also involves the heat source/sink aspect. Nonlinear system of ODEs (ordinary differential equations) is solved via HAM (homotopy analysis method). Interval of convergence for velocity and thermal fields is explicitly determined. Velocity, temperature and Nusselt number are examined under influential variables. Intensification in flow is observed with an increment in melting and wall thickness parameters. Temperature of fluid decays with higher melting, while the opposite trend holds for wall thickness parameter. Small Nusselt number is accounted for higher melting parameter, while it intensifies with larger velocity ratio parameter.

Keywords Stagnation point flow · Variable sheet thickness · Melting heat transfer · Oldroyd-B fluid · MHD · Heat source/sink

1 Introduction

Recently, transfer of heat in fluid flow by a stretchable sheet has an extensive range of applications. Such applications comprise metallic plates cooling, plastic sheets drawing, glass fibers, production of paper, spinning of metals, coating of fibers and wires, processing of chemical equipments, processing of food stuff, exchangers and processing of food stuff. All the processes of coating require a smoothy and glossy surface in order to fulfill the requirements for transparency, appearance, strength and low fraction. Viscous fluid flow by a stretchable surface is examined by Crane [1] for the first time. Turkyilmazoglu [2] inspected exact solution for couple stress fluid flow over a continuously stretchable sheet. Flow over a permeable stretchable sheet with thermal radiations and variable viscosity is investigated by Mukhopadhyay [3]. Nanofluid flow by a porous stretchable sheet is studied by Sheikholeslami et al. [4]. Hayat et al. [5] analyzed magnetohydrodynamic stagnation point flow of Jeffrey fluid toward a heated stretchable surface. Abbas et al. [6] inspected transfer of heat in viscous fluid flow by a porous stretchable/shrinkable cylinder. MHD steady flow of third-grade fluid over a stretchable cylinder is presented by Hayat et al. [7]. Hayat et al. [8] considered the revised Fourier heat flux model in flow of Jeffrey liquid with variable characteristics of thermal conductivity. Autocatalysis in MHD flow of Casson material is studied by Khan et al. [9]. Irreversibility in nanomaterial flow of viscous liquid is scrutinized by Hayat et al. [10]. Hayat et al. [11] examined the combined aspects of nonlinear radiation and mixed convection. Analysis of stretched flow of Sisko liquid with chemical reaction is performed by Hayat et al. [12]. Aziz et al. [13] performed the numerical study of heat source and sink in the rotatory flow of nanofluid. Darcy–Forchheimer 3D flow of nanofluid with convective boundary condition and chemical reactions is analyzed by Hayat et al. [14].

In thermal physics the fact of heat transfer is reported as the passage of thermal energy from the hot bodies to the cold one. This aspect in fluid mechanics has gained a particular

Technical Editor: Cezar Negrao, PhD.

✉ Khursheed Muhammad
kmuhammad@math.qau.edu.pk; khursheedfaiq@gmail.com

[1] Department of Mathematics, Quaid-I-Azam University (QAU), Islamabad 44000, Pakistan

[2] Nonlinear Analysis and Applied Mathematics (NAAM) Research Group, Department of Mathematics, Faculty of Science, King Abdulaziz University, Jeddah, Saudi Arabia

[3] Department of Mathematics, COMSATS Institute of Information Technology, Islamabad 44000, Pakistan

interest in engineering and industrial processes. Melting heat transport is introduced due to its relevance to some particular engineering problems such as magma solidification, melting of permafrost and preparations of semiconductor materials. At high heat flux for rapid cooling, ice slurries (a mixture of water and ice particles) could be utilized due to its high heat capacity because of its latent heat and direct contact heat transfer between heated surface and ice particles. Ice slurries can be used in order to regulate amorphous solids production, at low-temperature biomaterials and foods preservation, the properties of materials by thermal treatments such as quenching and in the emergency cooling system of nuclear reactors. Applications of melting heat transfer include oil extraction, silicon wafer process and thermal insulation, geothermal recovery. By placing ice slub in hot air stream the phenomenon of melting is studied by Robert [15]. Hayat et al. [16] inspected melting effect in flow of nanotubes by a variable thickness surface. Heat transfer via melting in micropolar fluid flow by a stretchable sheet is inquired by Yacob et al. [17]. Hayat et al. [18] explored heat transfer via melting in chemically reactive flow of nanotubes. An experiment for heat transfer via melting of the solid–liquid phase material paraffin added with nanoparticles in a vertically square enclosure is performed by Ho and Gao [19]. Das [20] inquired transfer of heat during the melting process of steady viscous fluid with MHD over a movable surface.

Magnetofluiddynamics is a field in which the motion of fluid (conducting electrically like liquid metals, salt water and plasmas) is analyzed. The word magnetohydrodynamics is the combination of three words. (1) Magneto means magnetic field, (2) hydro means water, and (3) dynamics is the movement of particles. In dynamic fluids flow, magnetic field induces current and produces forces on the fluid. Due to wide range of applications magnetohydrodynamics (MHD) is an important area of study for the scientists and engineers. MHD has been a subject of interest due to its significance in various fields arising from several natural phenomena like astrophysics, geophysics and many engineering processes such as confinement of plasma, liquid–metal cooling of nuclear reactors. There are huge applications of MHD technologies to the aerospace vehicles. One of these applications is to control the flow around reentry vehicles with MHD interactions. A shock wave is induced where the air pressure can exceed 10,000 k with high electrical conductivity. Then the magnetic field is applied externally, and the MHD interaction pushes the shock wave away from the vehicle and reduces the thermal flux on the wall. Hayat et al. [21] addressed the transfer of heat during melting in the flow of Burgers material over a stretching sheet. Irreversibility in MHD flow of viscous fluid by a rotating disk is elaborated by Rashidi et al. [22]. Mukhopadhyay [23] examined heat transfer in MHD flow over a stretchable sheet. Rashidi et al. [24] studied buoyancy, magnetic and thermal radiation effect in flow of nanofluid. Joule heating, partial slip and viscous dissipation effects on MHD nanofluid flow are explored by Hayat et al. [25]. Turkyilmazoglu [26] addressed the MHD flow of viscoelastic fluids by a stretchable/shrinkable sheet. Series solution for Falkner–Skan flow of MHD fluid is constructed by Abbasbandy and Hayat [27]. Free convective micropolar fluid flow is elaborated by Mishra et al. [28]. MHD nanofluid flow over a variable thickness surface is addressed by Hayat et al. [29]. Azeany et al. [30] analyzed the stagnation point flow bounded by a permeable stretchable surface. Khan et al. [31] presented viscous dissipative flow with chemical reactions. Thermo-hydrodynamic stability in water-based nanoliquid under the impact of transverse magnetic field is addressed by Wakif et al. [32]. Nanofluid flow of Powell-Eyring fluid due to a curved surface is considered by Hayat et al. [33]. Qayyum et al. [34] analyzed third-grade nanofluid flow over a variable thickness surface with convection. Non-uniform heat source/sink in flow of viscoelastic fluid with porous medium is done by Mishra et al. [35]. Chemical reactions with magnetic effects in flow of micropolar fluid are considered by Hayat et al. [36]. Joule heating in chemically reactive and radiative flow is elaborated by Shamshuddin et al. [37]. Bhukta et al. [38] examined mixed convective and dissipative flow with non-uniform heat source/sink. Non-Newtonian fluid over a permeable stretchable surface with exothermal reaction is analyzed by Eid et al. [39]. Baag et al. [40] analyzed buoyancy effects in MHD flow with heat source and sink.

The theme of present effort is to inspect heat transfer via melting in flow of MHD Oldroyd-B fluid, in the region of orthogonal stagnation point over a variable thicked surface. In addition, heat source/sink is also taken into account. Series solution via HAM (homotopy analysis method) [41–55] is constructed. Flow, temperature and local Nusselt number are explored graphically.

2 Mathematical formulation

We are interested in examining the stagnation point flow of an Oldroyd-B material toward a stretchable sheet of variable thickness. Melting heat transfer over sheet is considered. Sheet thickness is specified by $y = B(x+b)^{\frac{1-n}{2}}$. The effect of heat source/sink is also taken into account. We have considered that $T_\infty > T_n$. A transverse applied magnetic field conducts the flow. In Cartesian coordinate system x-axis is assumed along the surface, while y-axis is normal to flow. Under boundary layer assumptions ($o(x) = o(u) = o(1)$, $o(y) = o(v) = o(\delta)$) the conservation laws yield

$$\frac{\partial u}{\partial x} + \frac{\partial v}{\partial y} = 0, \tag{1}$$

$$
\begin{aligned}
&u\frac{\partial u}{\partial x}+v\frac{\partial u}{\partial y}+\lambda_1\left(u^2\frac{\partial^2 u}{\partial x^2}+v^2\frac{\partial^2 u}{\partial y^2}+2uv\frac{\partial^2 u}{\partial x\partial y}\right)\\
&=U_e\frac{dU_e}{dx}+\lambda_1 U_e^2\frac{d^2U_e}{dx^2}+\upsilon\frac{\partial^2 u}{\partial y^2}\\
&+\upsilon\lambda_2\left(u\frac{\partial^3 u}{\partial x\partial y^2}+v\frac{\partial^3 u}{\partial y^3}-\frac{\partial u}{\partial x}\frac{\partial^2 u}{\partial y^2}-\frac{\partial u}{\partial y}\frac{\partial^2 u}{\partial y^2}\right)\\
&-\frac{\sigma B_0^2}{\rho}\left(u-U_e+\upsilon\lambda_1\frac{\partial u}{\partial y}\right),
\end{aligned}
\tag{2}
$$

$$
u\frac{\partial T}{\partial x}+v\frac{\partial T}{\partial y}=\alpha\frac{\partial^2 T}{\partial y^2}+\frac{Q_0\left(T-T_n\right)}{\rho c_p},
\tag{3}
$$

with subjected boundary conditions

$$
u=U_w(x)=U_0(x+b)^n,\ v=0,\ T=T_n,\ \text{at}\ y=B(x+b)^{\frac{1-n}{2}},
$$

$$
u\to U_e(x)=U_\infty(x+b)^n,\ T\to T_\infty,\ \text{as}\ y\to\infty.
\tag{4}
$$

Melting condition for heat transfer is

$$
k\left(\frac{\partial T}{\partial y}\right)\Big|_{y=B(x+b)^{\frac{1-n}{2}}}=\rho\left[\lambda+C_s(T_n-T_0)\right]v(x,y)\Big|_{y=B(x+b)^{\frac{1-n}{2}}}.
\tag{5}
$$

Transformations are defined as follows:

$$
\begin{aligned}
\eta&=y\sqrt{\frac{n+1}{2}\frac{U_0(x+b)^{n-1}}{\upsilon}},\\
\psi&=\sqrt{\frac{2}{n+1}\upsilon U_0(x+b)^{n+1}}F(\eta),\ \Theta(\eta)\\
&=\frac{T-T_n}{T_\infty-T_n},\ u=U_0(x+b)^nF'(\eta),\\
v&=-\sqrt{\frac{n+1}{2}\upsilon U_0(x+b)^{n-1}}\\
&\left[F(\eta)+\eta F'(\eta)\frac{n-1}{n+1}\right].
\end{aligned}
\tag{6}
$$

After the application of these transformations continuity equation is trivially satisfied, while Eqs. (2-4) yield

$$
\begin{aligned}
&F'''+FF''-\frac{2n}{n+1}F'^2+\frac{2n}{n+1}A^2-\frac{2}{n+1}\\
&HF'+\frac{2}{n+1}HA+\beta_1((3n-1)\\
&FF'F''-\frac{2n(n-1)}{n+1}F'^3+\eta\frac{n-1}{2}F'^2F''-\frac{n+1}{2}\\
&F^2F'''-\frac{2n(n-1)}{n+1}A^3+\eta\frac{n-1}{n+1}HF'F''+HFF'')\\
&+\beta_2\left(\frac{3n-1}{2}F''^2-\frac{n+1}{2}FF^{(iv)}+(n-1)F'F'''\right)=0,
\end{aligned}
\tag{7}
$$

$$
\Theta''+\Pr\left(F\Theta'+\frac{2}{n+1}\delta\,\Theta\right)=0.
\tag{8}
$$

The boundary conditions now become

$$
\begin{aligned}
&F'(\alpha)=1,\ \Theta(0)=0,\ M\Theta'(\alpha)\\
&+\Pr\left[F(\alpha)+\frac{n-1}{n+1}\alpha\right]=0\ \text{at}\ \alpha\\
&=B\sqrt{\frac{n+1}{2}\frac{U_0}{\nu_f}},
\end{aligned}
$$

$$
F'(\infty)\to A,\ \Theta(\infty)\to 1,\ \text{as}\ \alpha\to\infty.
\tag{9}
$$

These definitions are

$$
\begin{aligned}
&M=\frac{C_{pf}\left(T_\infty-T_m\right)}{\lambda+C_s\left(T_m-T_0\right)},\ \Pr=\frac{\mu c_p}{k},\ A=\frac{U_\infty}{U_0},\\
&H=\frac{B_0^2\sigma}{\rho U_o},\ \eta=\alpha=B\sqrt{\frac{n+1}{2}\frac{U_0}{\upsilon}},\\
&\beta_1=\lambda_1U_0(x+b)^{n-1},\ \beta_2=\lambda_2U_0(x+b)^{n-1},\\
&\alpha=B\sqrt{\frac{n+1}{2}\frac{U_0}{\nu_f}}\ \text{and}\ \delta=\frac{Q_0}{\rho c_pU_o}.
\end{aligned}
\tag{10}
$$

Differentiation with respect to η is denoted by prime. We define $F(\eta)=f(\eta-\alpha)=f(\zeta)$, and Eqs. (8)–(10) become

$$
\begin{aligned}
&f'''+ff''-\frac{2n}{n+1}f'^2+\frac{2n}{n+1}A^2-\frac{2}{n+1}\\
&Hf'+\frac{2}{n+1}HA+\beta_1((3n-1)\\
&ff'f''-\frac{2n(n-1)}{n+1}f'^3+(\zeta+\alpha)\frac{n-1}{2}f'^2\\
&f''-\frac{n+1}{2}f^2f'''-\frac{2n(n-1)}{n+1}A^3+(\zeta+\alpha)\frac{n-1}{n+1}\\
&Hf'f''+Hff'')\\
&+\beta_2\left(\frac{3n-1}{2}f''^2-\frac{n+1}{2}ff^{(iv)}+(n-1)f'f'''\right)=0,
\end{aligned}
\tag{11}
$$

$$
\theta''+\Pr\left(f\theta'+\frac{2}{n+1}\delta\,\theta\right)=0,
\tag{12}
$$

$$
f'(0)=1,\ \theta(0)=0,\ M\,\theta'(0)+\Pr\left[f(0)+\frac{n-1}{n+1}\alpha\right]=0,
$$

$$
f'(\infty)\to A,\ \theta(\infty)\to 1,\ \text{as}\ \zeta\to\infty.
\tag{13}
$$

Local Nusselt number (Nu_x) is

$$
Nu_x=\frac{(x+b)\,q_w}{k(T_\infty-T_n)},
$$

$$q_w = -\kappa \left(\frac{\partial T}{\partial y} \right)_{y=B(x+b)^{\frac{1-n}{2}}}. \tag{14}$$

Dimensionless local Nusselt numbers are reduced to

$$Nu_x Re_x^{-1/2} = -\sqrt{\frac{n+1}{2}}\theta'(0), \tag{15}$$

where local Reynolds number is $Re_x = \frac{U_w(x+b)}{\upsilon}$.

2.1 Solutions via homotopy

Initial guesses along with auxiliary linear operators are

$$f_0(\zeta) = A\zeta + (1-A)(1-\exp(-\zeta)) - \frac{M}{\Pr} + \alpha\frac{n-1}{n+1},$$

$$\theta_0(\zeta) = 1 - \exp(-\zeta),$$

$$\mathbf{L}_f(f) = \frac{d^3 f}{d\zeta^3} - \frac{df}{d\zeta},$$

$$\mathbf{L}_\theta(\theta) = \frac{d^2\theta}{d\zeta^2} - \theta. \tag{16}$$

Zeroth- and mth-order deformation problems are as follows.

2.2 Problem of zeroth order

$$(1-p)\,\mathbf{L}_f[\hat{f}(\zeta;p) - f_0(\zeta)] = p\hbar_f \mathbf{N}_f[\hat{f}(\zeta;p), \hat{\theta}(\zeta;p)], \tag{17}$$

$$(1-p)\,\mathbf{L}_\theta[\hat{\theta}(\zeta;p) - \theta_0(\zeta)] = p\hbar_\theta \mathbf{N}_\theta[\hat{\theta}(\zeta;p), \hat{f}(\zeta;p)], \tag{18}$$

$$\hat{f}'(0;p) = 1, \quad \hat{f}'(\infty;p) \to A, \tag{19}$$

$$\hat{\theta}'(0;p) = -\frac{\Pr}{M}\left(\widehat{f}(0;p) + \frac{m-1}{m+1}\alpha\right), \quad \hat{\theta}(\infty;p) \to 1. \tag{20}$$

$$\begin{aligned}
N_f\left[\hat{f}(\zeta, p)\right] = {} & \frac{\partial^3 \hat{f}(\zeta;p)}{\partial\zeta^3} + \widehat{f}(\zeta;p)\frac{\partial^2 \hat{f}(\zeta;p)}{\partial\zeta^2} \\
& - \frac{2n}{n+1}\left(\frac{\partial \hat{f}(\zeta;p)}{\partial\zeta}\right)^2 + \frac{2n}{n+1}A^2 - \frac{2}{n+1}H\frac{\partial \hat{f}(\zeta;p)}{\partial\zeta} \\
& + \beta_1((3n-1)\hat{f}(\zeta;p)\frac{\partial \hat{f}(\zeta;p)}{\partial\zeta}\frac{\partial^2 \hat{f}(\zeta;p)}{\partial\zeta^2} - \frac{2n(n-1)}{n+1}\left(\frac{\partial \hat{f}(\zeta;p)}{\partial\zeta}\right)^3 \\
& + \frac{2}{n+1}HA + (\zeta+\alpha)\frac{n-1}{2}\left(\frac{\partial \hat{f}(\zeta;p)}{\partial\zeta}\right)^2\frac{\partial^2 \hat{f}(\zeta;p)}{\partial\zeta^2} \\
& - \frac{n+1}{2}\left(\hat{f}(\zeta;p)\right)^2\frac{\partial^3 \hat{f}(\zeta;p)}{\partial\zeta^3} - \frac{2n(n-1)}{n+1}A^3 \\
& + \left(\zeta+\alpha)\frac{n-1}{n+1}H\frac{\partial \hat{f}(\zeta;p)}{\partial\zeta}\frac{\partial^2 \hat{f}(\zeta;p)}{\partial\zeta^2}H\hat{f}(\zeta;p)\frac{\partial \hat{f}(\zeta;p)}{\partial\zeta^2}\right) \\
& + \beta_2\left(\frac{3n-1}{2}\left(\frac{\partial^2 \hat{f}(\zeta;p)}{\partial\zeta^2}\right)^2 - \frac{n+1}{2}\hat{f}(\zeta;p)\frac{\partial^4 \hat{f}(\zeta;p)}{\partial\zeta 4} + (n-1)\frac{\partial \hat{f}(\zeta;p)}{\partial\zeta}\frac{\partial^3 \hat{f}(\zeta;p)}{\partial\zeta^3}\right),
\end{aligned} \tag{21}$$

$$\mathbf{N}_\theta\left[\hat{\theta}(\zeta;p), \hat{f}(\zeta;p)\right] = \frac{\partial^2\hat{\theta}(\zeta,p)}{\partial\zeta^2} + \Pr\left(\hat{f}(\zeta;p)\frac{\partial\hat{\theta}(\zeta,p)}{\partial\zeta} + \frac{2}{n+1}\delta\,\hat{\theta}(\zeta,p)\right). \tag{22}$$

Here $p \in [0,\ 1]$ depicts embedding parameter.

2.3 Problem of mth order

$$\mathbf{L}_f[f_m(\zeta) - \chi_m f_{m-1}(\zeta)] = \hbar_f \mathbf{R}_m^f(\zeta), \tag{23}$$

$$\mathbf{L}_\theta[\theta_m(\zeta) - \chi_m \theta_{m-1}(\zeta)] = \hbar_\theta \mathbf{R}_m^\theta(\zeta), \tag{24}$$

$$f_m'(0) = 0,\ \theta_m(0) = 0,\ \theta_m'(0) = -\frac{\Pr}{M}f_m(0),$$

$$f_m'(\infty) \to 0,\ \ \theta_m(\infty) \to 0. \tag{25}$$

$$\begin{aligned}
\mathbf{R}_m^f(\eta) = {} & f_{m-1}''' + \sum_{k=0}^{m-1}\left(f_{m-1-k}f_k''\right) \\
& - \frac{2n}{n+1}\sum_{k=0}^{m-1}\left(f_{m-1-k}'f_k'\right) + \frac{2n}{n+1}A^2\left(1-\chi_m\right) \\
& - \frac{2}{n+1}Hf_{m-1}' + \frac{2}{n+1}HA\left(1-\chi_m\right) \\
& + H\sum_{k=0}^{m-1}(f_k f_{m-1-k}') + \beta_1((3n-1) \\
& \sum_{k=0}^{m-1}(f_{m-1-k}\sum_{l=0}^{k}\left(f_{k-l}'f_l''\right) - \frac{2n(n-1)}{n+1}f_{m-1-k}' \\
& \sum_{l=0}^{k}\left(f_{k-l}'f_l'\right) + (\zeta+\alpha)\frac{n-1}{2}f'\sum_{l=0}^{k}\left(f_{k-l}'f_l''\right) + \beta_1((3n-1) \\
& \sum_{k=0}^{m-1}(f_{m-1-k}\sum_{l=0}^{k}\left(f_{k-l}'f_l''\right) - \frac{2n(n-1)}{n+1}f_{m-1-k}' \\
& \sum_{l=0}^{k}\left(f_{k-l}'f_l'\right) + (\zeta+\alpha)\frac{n-1}{2}f'\sum_{l=0}^{k}\left(f_{k-l}'f_l''\right) - \frac{n+1}{2}f_{m-1-k}\sum_{l=0}^{k} \\
& \left(f_{k-l}f_l'''\right)) - \frac{2n(n-1)}{n+1}A^3\left(1-\chi_m\right) + (\zeta+\alpha)\frac{n-1}{n+1}H\sum_{k=0}^{m-1}\left(f_{m-1-k}'f_k''\right) \\
& + H\sum_{k=0}^{m-1}\left(f_{m-1-k}f_k''\right)) \\
& + \beta_2\left(\frac{3n-1}{2}\sum_{k=0}^{m-1}\left(f_{m-1-k}''f_k''\right) - \frac{n+1}{2}\sum_{k=0}^{m-1}\left(f_{m-1-k}f_k^{(iv)}\right) + (n-1)\sum_{k=0}^{m-1}\left(f_{m-1-k}'f_k'''\right)\right),
\end{aligned} \tag{26}$$

$$\mathbf{R}_m^\theta(\eta) = \theta_{m-1}'' + \Pr\left(\sum_{k=0}^{m-1}\left(f_{m-1-k}\theta_k'\right) + \frac{2}{n+1}\delta\,\theta_{m-1}\right), \tag{27}$$

$$\chi_m = \begin{cases} 0, & m \le 1 \\ 1, & m > 1. \end{cases} \tag{28}$$

As we vary p from 0 to 1, $\hat{f}(\zeta;p)$ and $\hat{\theta}(\zeta;p)$ vary from the initial solutions $f_0(\zeta)$ and $\theta_0(\zeta)$ to the final solutions $f(\zeta)$ and $\theta(\zeta)$, respectively. Thus,

$$\hat{f}(\zeta;0) = f_0(\zeta),\ \hat{f}(\zeta;1) = f(\zeta), \tag{29}$$

$$\hat{\theta}(\zeta;0) = \theta_0(\zeta),\ \hat{\theta}(\zeta;1) = \theta(\zeta). \tag{30}$$

By means of Taylor series expansion we have

$$\hat{f}(\zeta;p) = f_0(\zeta) + \sum_{m=1}^{\infty} f_m(\zeta)p^m,\ f_m(\zeta) = \frac{1}{m!}\frac{\partial^m \hat{f}(\zeta;p)}{\partial p^m}\bigg|_{p=0}, \tag{31}$$

$$\hat{\theta}(\zeta;p) = \theta_0(\zeta) + \sum_{m=1}^{\infty} \theta_m(\zeta)p^m,\ \theta_m(\zeta) = \frac{1}{m!}\frac{\partial^m \hat{\theta}(\zeta;p)}{\partial p^m}\bigg|_{p=0}. \tag{32}$$

Also

$$f(\zeta) = f_0(\eta) + \sum_{m=1}^{\infty} f_m(\zeta), \tag{33}$$

$$\theta(\eta) = \theta_0(\zeta) + \sum_{m=1}^{\infty} \theta_m(\zeta). \tag{34}$$

The general solutions f_m and θ_m are

$$f_m(\zeta) = f_m^*(\zeta) + A_1 + A_2 e^{\zeta} + A_3 e^{-\zeta}, \tag{35}$$

$$\theta_m(\zeta) = \theta_m^*(\zeta) + A_4 e^{\zeta} + A_5 e^{-\zeta}, \tag{36}$$

where f_m^* and $\theta_m'^*$ depict special solutions and $A_i (i = 1, 2, \dots, 5)$ represent arbitrary constants. Thus, we have

$$A_1 = \frac{M}{\mathrm{Pr}}\left(A_5 - \theta_m'^*(0)\right) - A_3 - f_m^*(0), \\ A_2 = A_4 = 0,\ A_3 = f_m^{*'}(0), A_5 = -\theta_m^*(0). \tag{37}$$

2.4 Convergence analysis

For $\hbar_f$ and $\hbar_\theta$, $\hbar$-curves are displayed in Figs. 1 and 2. The acceptable ranges of $\hbar_f$ and $\hbar_\theta$ are $-1.45 \le \hbar_f \le -1.1$ and $-1.3 \le \hbar_\theta \le -0.68$.

3 Discussion

This section intends to study the influences of different pertinent variables on flow and temperature. The effect of M on flow is portrayed in Fig. 3. Clearly, both velocity and associated penetration depth are enhanced for higher M. It is due to enhancement of convective flow from heated flow in direction of cold melting surface. Hence, fluid velocity intensifies. Figure 4 displays the outcome of A on velocity. Interestingly, the velocity enhances for both $A > 1$ and $A < 1$. The penetration depth has reverse behavior for higher $A > 1$ and $A < 1$. No boundary layer exists when $A = 1$. Figure 5 shows the impact of α on velocity. Increment in velocity

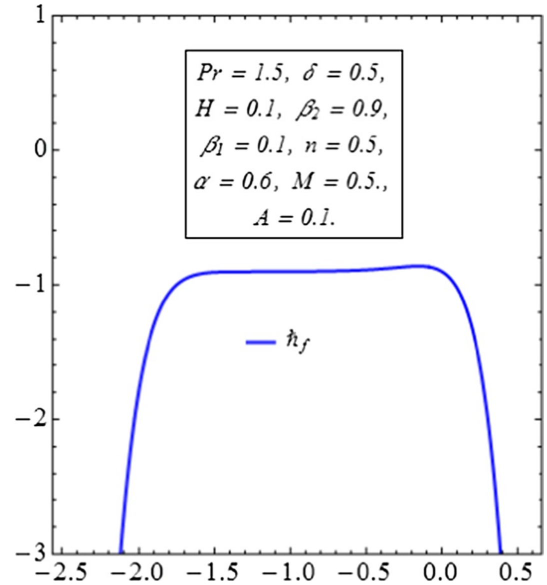

Fig. 1 Sketch for $\hbar_f$

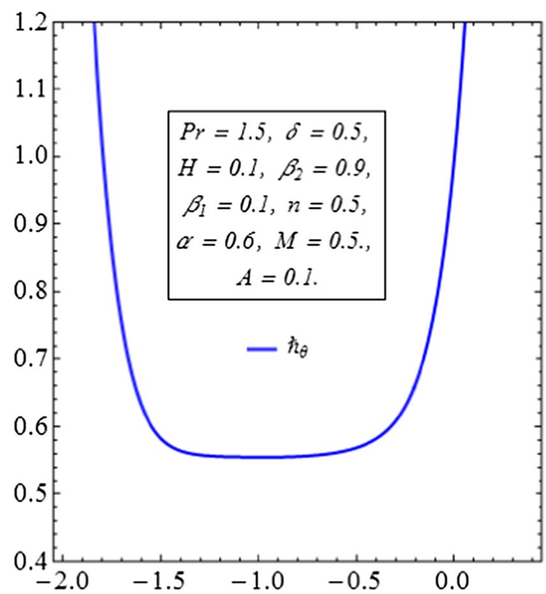

Fig. 2 Sketch for $\hbar_\theta$

is found out for larger α. Figure 6 shows the influence of β_1 on the velocity profile. Here velocity decays for higher β_1. Figure 7 shows the influence of H on velocity distribution. Interestingly, velocity and momentum layer thickness decrease for higher H. In fact, larger H is responsible for the increase in Lorentz force (resistive force). Hence, for higher H, velocity decreases. Velocity under the impact of β_2 is labeled in Fig. 8. It is concluded that both flow and penetration depth intensify with an increase in β_2. The effect of n on

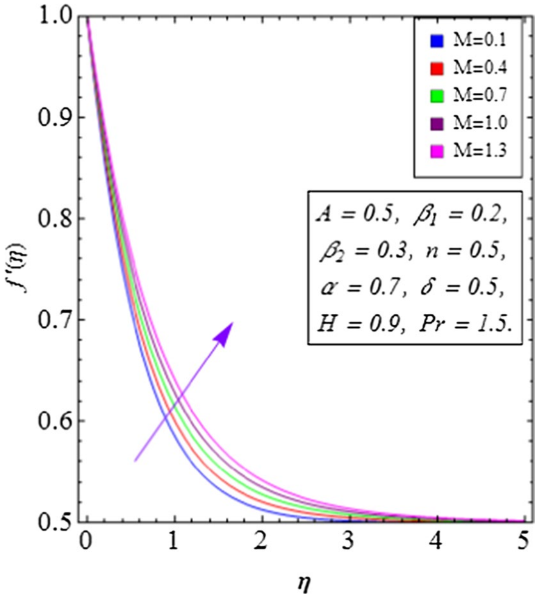

Fig. 3 Variations in f' via M

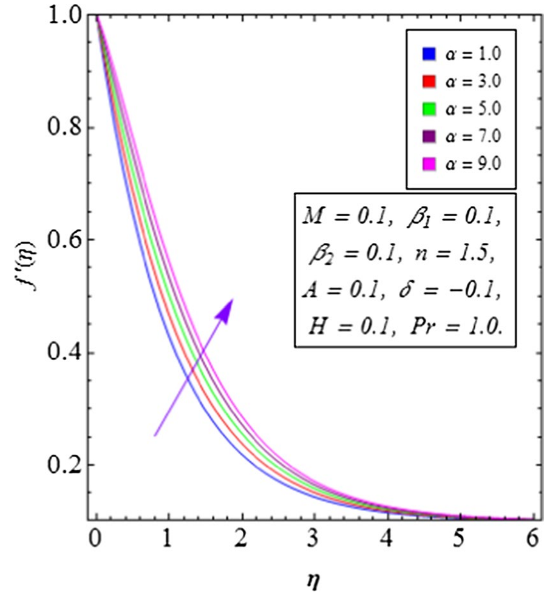

Fig. 5 Variations in f' via α

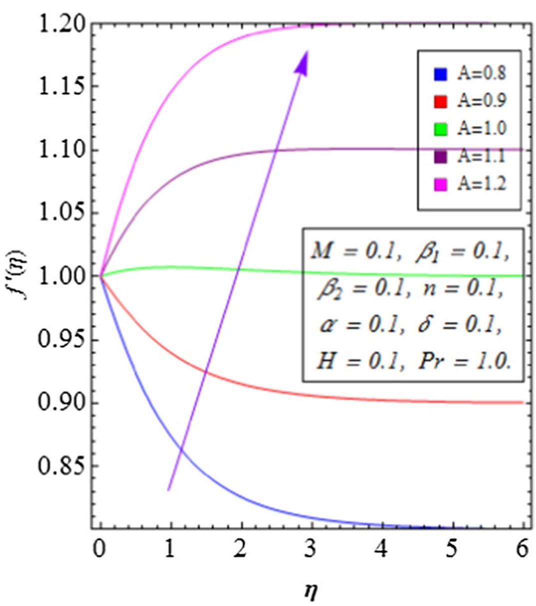

Fig. 4 Variations in f' via A

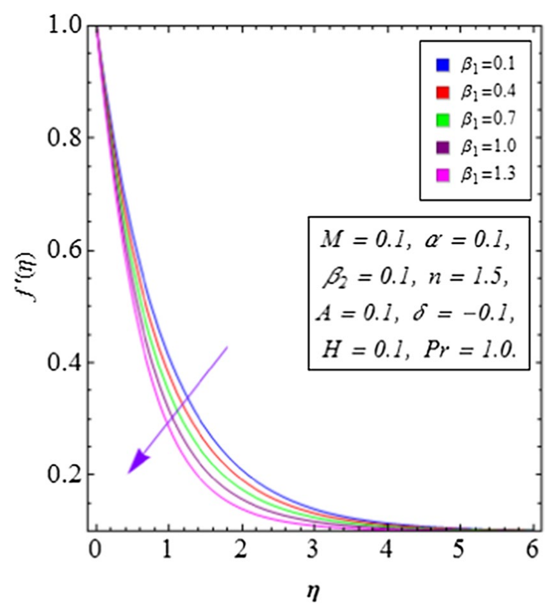

Fig. 6 Variations in f' via β_1

flow is drawn in Fig. 9. The parameter n has three important equities: controlling (1) shape of sheet, (2) motion of the fluid and (3) boundary layer behavior. State (shape) of the sheet highly depends on the parameter n such that surface is flat for $n = 1$, enhancement of α occurs for $n < 1$ which corresponds to outer convex-type shape of the sheet, and $n > 1$ corresponds to decrease in α and inner convex-type shape of the sheet. Boundary layer behavior can also be determined by means of this parameter such that for $n = 1$, we have $f(0) = 0$, which represents that the sheet is impermeable. Similarly, for $n > 1$ and $n < 1$, we have $f(0) > 1$ and $f(0) < 1$, which represent suction and blowing, respectively. For larger n $(n > 1)$, there is an enlargement in fluid velocity, while for $(n < 1)$ the decay in fluid velocity is observed. Figure 10

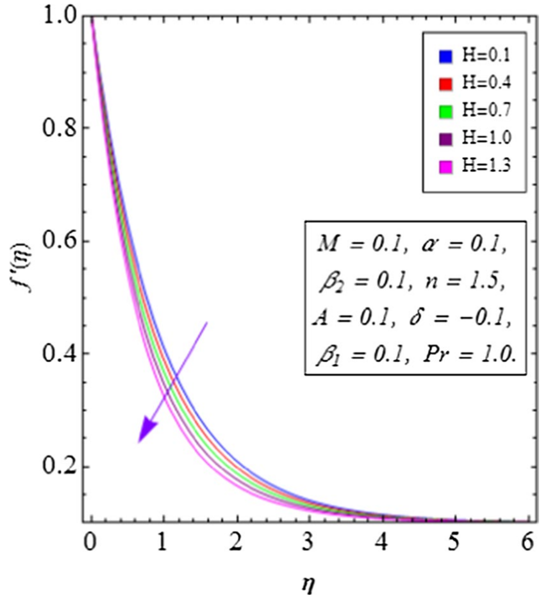

Fig. 7 Variations in f' via H

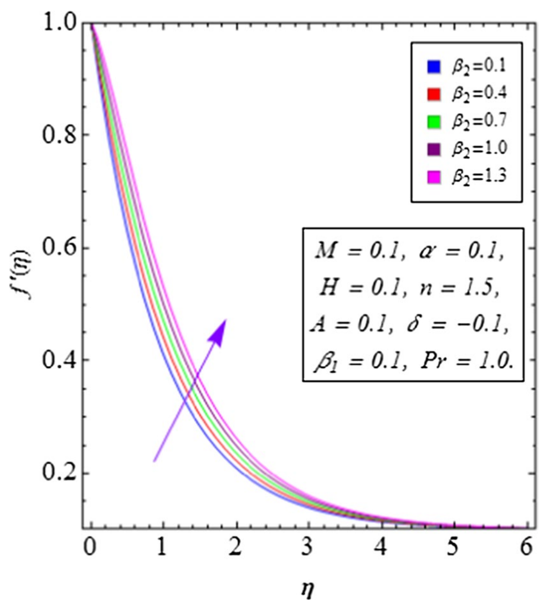

Fig. 8 Variations in f' via β_2

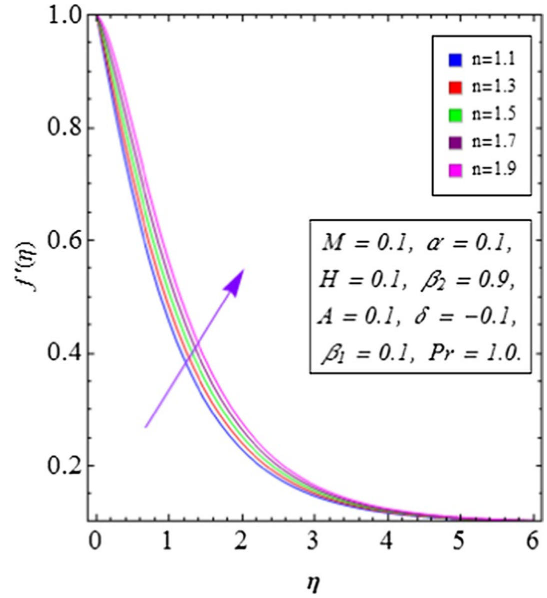

Fig. 9 Variations in f' via n

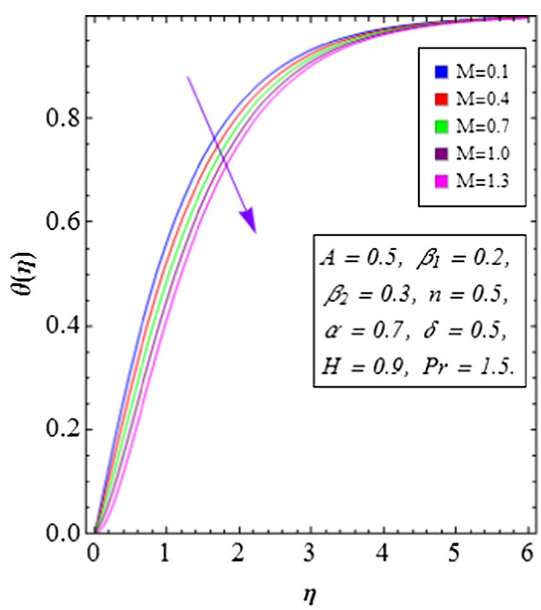

Fig. 10 Variations in θ via M

displays temperature against M. Here temperature decays when M increases. An increase in M leads to more flow toward melting surface from the heated fluid, which intensifies the fluid flow and temperature of the fluid decay. The impact of A on temperature is portrayed in Fig. 11. Intensification is observed in temperature for higher A. Also penetration depth corresponding to temperature decays for higher A. The effect of α on temperature of the fluid is portrayed in Fig. 12. Temperature reduces for larger wall thickness parameter. Figure 13 shows variation in temperature of fluid for higher δ. It is found that temperature shows increasing behavior for $\delta > 0$, while it decreases for $\delta < 0$. Figure 14 shows the impact of n on the temperature of the fluid. It is found that the temperature of the fluid decays for larger n.

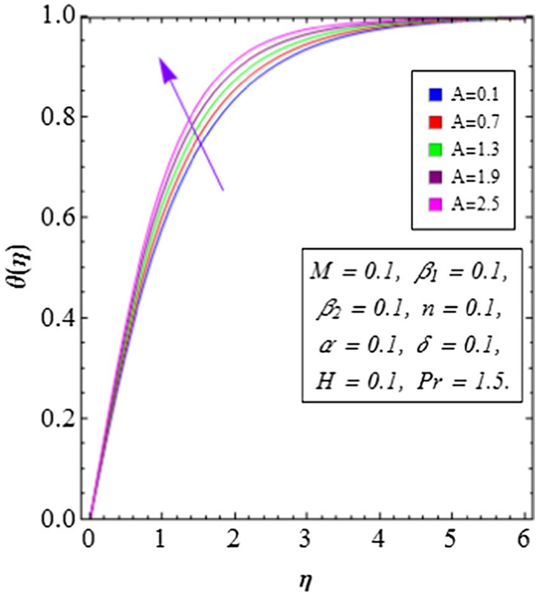

Fig. 11 Variations in θ via A

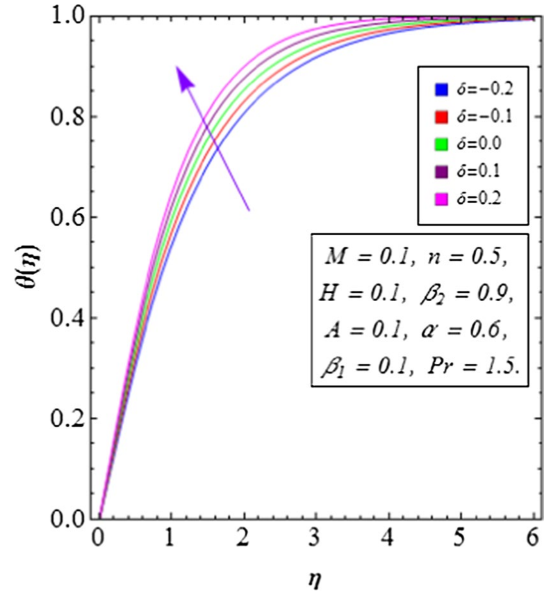

Fig. 13 Variations in θ via δ

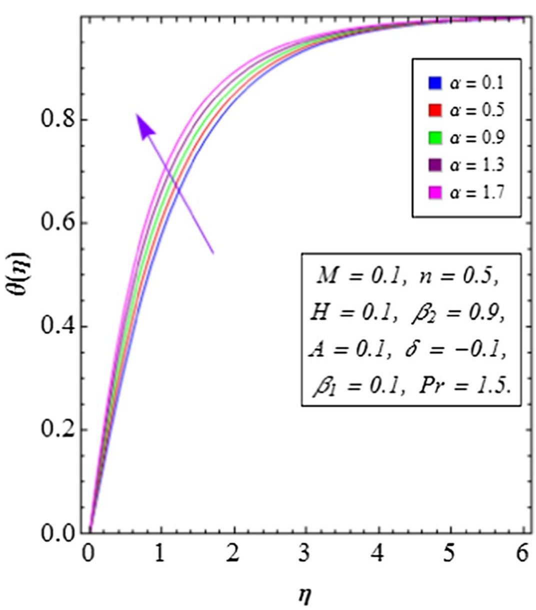

Fig. 12 Variations in θ via α

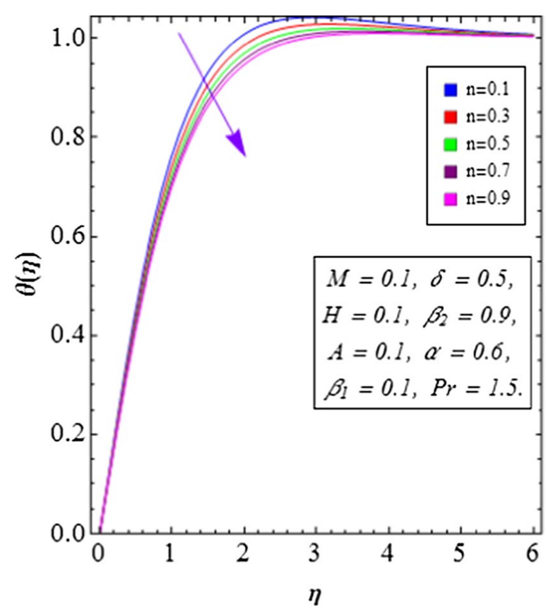

Fig. 14 Variations in θ via n

Figure 15 shows variation in Pr with respect to temperature. Here temperature enhances for higher values of Pr. Further, thermal penetration depth decays with an increase in Pr. Nusselt number is inspected under the influence of M, A and Pr. Decay in Nusselt number is found for larger M, while it indicates the opposite behavior for higher A and Pr. Table 1 gives the nomenclature of involved variables, while Table 2 gives the numerical evaluation of Nusselt number. Furthermore, comparison of Nusselt number corresponding to various values of A with published works [56, 57] in past is given in Table 3. Here an excellent agreement is noticed (Fig. 16a, b).

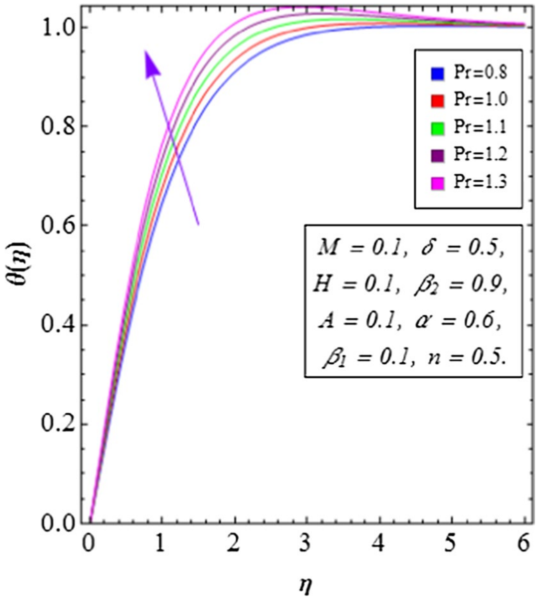

Fig. 15 Variations in θ via Pr

Table 2 Numerical evaluation of Nusselt number for higher M, A and Pr when $\delta = 0.1$, $H = 0.1$, $n = 0.5$ and $\alpha = 0.6$

M	A	Pr	$-\sqrt{\frac{n+1}{2}}\theta'(0)$
0.1	0.5	1.5	0.9399
0.2			0.9386
0.3			0.8842
0.4			0.8345
0.1	1.0	1.5	0.8552
	2.0		0.9731
	3.0		1.2860
	4.0		1.7539
0.1	0.5	0.5	0.5103
		1.0	0.7664
		1.5	0.9399
		2.0	1.2140

Table 3 Comparison of Nusselt number with published works for various values of A when $\mathrm{Pr} = 1 = n$, while all other parameters are zero

A	[56]	[57]	Current results
0.1	0.603	0.600	0.601
0.2	0.625	0.621	0.622
0.5	0.692	0.689	0.691
1.0	0.796	0.793	0.795
2.0	0.974	0.971	0.973
3.0	1.124	1.122	1.123

4 Concluding remarks

We disclosed the characteristics of MHD flow of a non-Newtonian (Oldroyd-B) fluid. Flow is considered over a stretchable sheet of variable thickness in region of stagnation point. Key points are as follows:

- Velocity shows intensification with larger M, α and β_2, while it decays with an increase in H, n and β_1.
- Higher M, $\delta > 0$ (heat source parameter) and Pr are responsible for the reduction in temperature, but the opposite behavior is found for larger n and α.
- Rate of heat transfer or process of cooling can be intensified by using larger A and Pr, while it decays for higher M.

Table 1 Nomenclature of involved parameters

Nomenclature			
u, v	Velocity components	U_w	Stretching velocity
T_∞	Ambient temperature	U_0, U_∞	Reference velocities
T_n	Wall temperature	λ_1	Relaxation time
B_0	Strength of magnetic field	λ_2	Retardation time
β_1	Deborah number due to relaxation time	Ue	Free stream velocity
α_f	Thermal diffusivity of base fluid	ρ	Fluid density
n	Shape parameter	c_p	Specific heat of fluid
σ	Electric conductivity	λ	Latent heat
C_s	Heat capacity of solid surface	δ	Heat source/sink parameter
M	Melting parameter	Pr	Prandtl number
H	Magnetic parameter	A	Velocity ratio parameter
β_2	Deborah number due to retardation time	f'	Dimensionless velocity
$\hbar_f$, $\hbar_\theta$	Convergence control parameters	θ	Dimensionless temperature

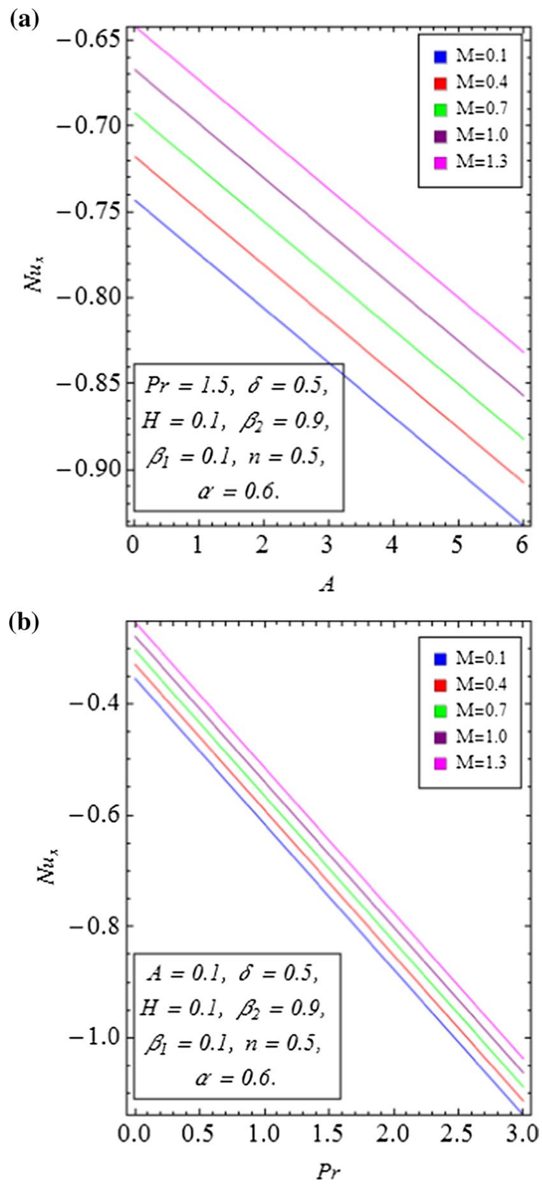

Fig. 16 **a** Variations in Nu_x via M and A. **b** Variations in Nu_x via M and Pr

References

1. Crane LJ (1970) Flow past a stretching plate. Z Angew Math Phys 21:645–647
2. Turkyilmazoglu M (2014) Exact solutions for two-dimensional laminar flow over a continuously stretching or shrinking sheet in an electrically conducting quiescent couple stress fluid. Int J Heat Mass Transf 72:1–8
3. Mukhopadhyay S (2013) Effects of thermal radiation and variable fluid viscosity on stagnation point flow past a porous stretching sheet. Meccanica 48:1717–1730
4. Shiekholeslami M, Ellahi R, Ashorynejad HR, Domairry G, Hayat T (2014) Effects of heat transfer in flow of nanofluids over a permeable stretching wall in a porous medium. J Comput Theor Nanos 11:486–496
5. Hayat T, Asad S, Mustafa M, Alsaedi A (2015) MHD stagnation-point flow of Jeffrey fluid over a convectively heated stretching sheet. Comput Fluids 108:179–185
6. Abbas Z, Rasool S, Rashidi MM (2015) Heat transfer analysis due to an unsteady stretching/shrinking cylinder with partial slip condition and suction. Ain Shams Eng J 6:939–945
7. Hayat T, Shafiq A, Alsaedi A (2015) MHD axisymmetric flow of third grade fluid by a stretching cylinder. Alexandria Eng J 54:205–212
8. Hayat T, Khan MI, Farooq M, Alsaedi A, Waqas M, Yasmeen T (2016) Impact of Cattaneo-Christov heat flux model in flow of variable thermal conductivity fluid over a variable thicked surface. Int J Heat Mass Transf 99:702–710
9. Khan MI, Waqas M, Hayat T, Alsaedi A (2017) A comparative study of Casson fluid with homogeneous-heterogeneous reactions. J Colloid Interface Sci 498:85–90
10. Hayat T, Khan MI, Qayyum S, Alsaedi A (2018) Entropy generation in flow with silver and copper nanoparticles. Colloid Surf A Physicoch Eng Aspect 539:335–346
11. Hayat T, Ullah I, Alsaedi A, Ahmad B (2018) Simultaneous effects of non-linear mixed convection and radiative flow due to Riga-plate with double stratification. J Heat Transf 140:102008
12. Hayat T, Ullah I, Alsaedi A, Ahmad B (2018) Numerical simulation for homogeneous–heterogeneous reactions in flow of Sisko fluid. J Braz Soc Mech Sci Eng 40:73
13. Aziz A, Alsaedi A, Muhammad T, Hayat T (2018) Numerical study for heat generation/absorption in flow of nanofluid by a rotating disk. Results Phys 8:785–792
14. Hayat T, Aziz A, Muhammad T, Alsaedi A (2018) An optimal analysis for Darcy-Forchheimer 3D flow of nanofluid with convective condition and homogeneous–heterogeneous reactions. Phys Lett A 382:2846–2855
15. Roberts L (1958) On the melting of a semi-infinite body of ice placed in a hot stream of air. J Fluid Mech 4:505–528
16. Hayat T, Muhammad K, Farooq M, Alsaedi A (2016) Melting heat transfer in stagnation point flow of carbon nanotubes towards variable thickness surface. AIP Adv 6:015214
17. Yacob NA, Ishak A, Pop I (2011) Melting heat transfer in boundary layer stagnation-point flow towards a stretching/shrinking sheet in a micropolar fluid. Comput Fluids 47:16–21
18. Hayat T, Muhammad K, Alsaedi A, Asghar S (2018) Numerical study for melting heat transfer and homogeneous-heterogeneous reactions in flow involving carbon nanotubes. Results Phys 8:415–421
19. Ho CJ, Gao JY (2013) An experimental study on melting heat transfer of paraffin dispersed with Al_2O_3 nanoparticles in a vertical enclosure. Int J Heat Mass Transf 62:2–8
20. Das K (2014) Radiation and melting effects on MHD boundary layer flow over a moving surface. Ain Shams Eng J 5:1207–1214
21. Awais M, Hayat T, Alsaedi A (2015) Investigation of heat transfer in flow of Burgers' fluid during a melting process. J Egypt Math Soci 23:410–415
22. Rashidi MM, Kavyani N, Abelman S (2014) Investigation of entropy generation in MHD and slip flow over a rotating porous disk with variable properties. Int J Heat Mass Transf 70:892–917
23. Mukhopadhyay S, Layek GC, Samad SA (2005) Study of MHD boundary layer flow over a heated stretching sheet with variable viscosity. Int J Heat Mass Transf 48:4460–4466
24. Rashidi MM, Vishnu Ganesh N, Abdul Hakeem AK, Ganga B (2014) Buoyancy effect on MHD flow of nanofluid over a stretching sheet in the presence of thermal radiation. J Mol Liquids 198:234–238
25. Hayat T, Nisar Z, Ahmad B, Yasmin H (2015) Simultaneous effects of slip and wall properties on MHD peristaltic motion of nanofluid with Joule heating. J Mag Mag Mater 395:48–58

26. Turkyilmazoglu M (2014) Three dimensional MHD flow and heat transfer over a stretching/shrinking surface in a viscoelastic fluid with various physical effects. Int. J. Heat Mass Transf 78:150–155
27. Abbasbandy S, Hayat T (2009) Solution of the MHD Falkner-Skan flow by homotopy analysis method. Commun Nonlinear Sci Numer Simul 14:3591–3598
28. Mishra SR, Pattnaik PK, Dash GC (2015) Effect of heat source and double stratification on MHD free convection in a micropolar fluid. Alexandria Eng J 54:681–689
29. Hayat T, Waqas M, Alsaedi A, Bashir G, Alzahrani F (2017) Magnetohydrodynamic (MHD) stretched flow of tangent hyperbolic nanoliquid with variable thickness. J Mol Liq 229:178–184
30. Azeany NA, Nasir M, Ishak A, Pop I (2017) Stagnation-point flow and heat transfer past a permeable quadratically stretching/shrinking sheet. Chin J Phys 55:2081–2091
31. Khan MI, Hayat T, Khan MI, Alsaedi A (2017) A modified homogeneous-heterogeneous reactions for MHD stagnation flow with viscous dissipation and Joule heating. Int J Heat Mass Transf 113:310–317
32. Wakif A, Boulahia Z, Mishra SR, Rashidi MM, Sehaqui R (2018) Influence of a uniform transverse magnetic field on the thermo-hydrodynamic stability in water-based nanofluids with metallic nanoparticles using the generalized Buongiorno's mathematical model. Eur Phys J Plus 133:181. https://doi.org/10.1140/epjp/i2018-12037-7
33. Hayat T, Sajjad R, Muhammad T, Alsaedi A, Ellahi R (2017) On MHD nonlinear stretching flow of Powell-Eyring nanomaterial. Results Phys 7:535–543
34. Qayyum S, Hayat T, Alsaedi A (2017) Chemical reaction and heat generation/absorption aspects in MHD nonlinear convective flow of third grade nanofluid over a nonlinear stretching sheet with variable thickness. Results Phys 7:2752–2761
35. Mishra SR, Tripathy RS, Dash GC (2018) MHD viscoelastic fluid flow through porous medium over a stretching sheet in the presence of non-uniform heat source/sink. Rendiconti del Circolo Matematico di Palermo Series 2(67):129–143
36. Hayat T, Sajjad R, Ellahi R, Alsaedi A, Muhammad T (2017) Homogeneous-heterogeneous reactions in MHD flow of micropolar fluid by a curved stretching surface. J Mol Liq 240:209–220
37. Shamshuddin MD, Mishra SR, Bég O, Kadir A Unsteady reactive magnetic radiative micropolar flow, heat and mass transfer from an inclined plate with joule heating: a model for magnetic polymer processing. Proc Inst Mech Eng Part C J Mech Eng Sci. https://doi.org/10.1177/0954406218768837
38. Bhukta D, Dash GC, Mishra SR, Baag S (2017) Dissipation effect on MHD mixed convection flow over a stretching sheet through porous medium with non-uniform heat source/sink. Ain Shams Eng J 8:353–361
39. Eid MR, Mishra SR (2017) Exothermically reacting of non-Newtonian fluid flow over a permeable non-linear stretching vertical surface with heat and mass fluxes. Comput Ther Sci Int J 9:283–296
40. Baag S, Mishra SR, Nayak B (2017) Buoyancy effects on free convective MHD flow in the presence of heat source/sink. Model Measur Control-B 86:14–32
41. Hayat T, Ullah I, Alsaedi A, Ahmad B (2017) Radiative flow of Carreau liquid in presence of Newtonian heating and chemical reaction. Results Phys 7:715–722
42. Liao SJ (2012) Homotopy analysis method in non-linear differential equations. Springer and Higher Education Press, Heidelberg
43. Hayat T, Khan MI, Farooq M, Alsaedi A, Waqas M, Yasmeen T Impact of Cattaneo–Christov heat flux model in flow of variable thermal conductivity fluid over a variable thicked surface. Int J Heat Mass Transf 99:702–710
44. Hussain T, Hayat T, Shehzad SA, Alsaedi A, Chen B (2015) A model of solar radiation and Joule heating in flow of third grade nanofluid. Z Naturfor-A 70:177–184
45. Abbasbandy S, Jalil M (2013) Determination of optimal convergence-control parameter value in homotopy analysis method. Numer Algor 64:593–605
46. Hayat T, Muhammad K, Muhammad T, Alsaedi A (2018) Melting heat in radiative flow of carbon nanotubes with homogeneous-heterogeneous reactions. Commun Theor Phys 69:441–448
47. Rashidi MM, Rostami B, Freidoonimehr N, Abbasbandy S (2014) Free convection heat and mass transfer for MHD fluid flow over a permeable vertical stretching sheet in the presence of the radiation and buoyancy effects. Ain Shams Eng J 5:901–912
48. Hayat T, Muhammad K, Farooq M, Alsaedi A (2016) Squeezed flow subject to Cattaneo-Christov heat flux and rotating frame. J Mol Liq 220:216–222
49. Han S, Zheng L, Li C, Zhang X (2014) Coupled flow and heat transfer in viscoelastic fluid with Cattaneo-Christov heat flux model. Appl Math Lett 38:87–93
50. Hayat T, Muhammad K, Farooq M, Alsaedi A (2016) Unsteady Squeezing Flow of Carbon Nanotubes with Convective Boundary Conditions. PLoS ONE 11:0152923
51. Hayat T, Rashid M, Imtiaz M, Alsaed A (2017) Nanofluid flow due to rotating disk with variable thickness and homogeneous-heterogeneous reactions. Int J Heat Mass Transf 113:96–105
52. Hayat T, Ullah I, Alsaedi A, Ahmad B (2017) Modeling tangent hyperbolic nanoliquid flow with heat and mass flux conditions. Eur Phys J Plus 132:112
53. Hayat T, Iqbal Z, Qasim M, Obaidat S (2018) Steady flow of an Eyring Powell fluid over a moving surface with convective boundary conditions. Int J Heat Mass Transf 55:1817–1822
54. Hayat T, Imtiaz M, Alsaedi A, Almezal S (2016) On Cattaneo-Christov heat flux in MHD flow of Oldroyd-B fluid with homogeneous–heterogeneous reactions. J Magn Magn Mater 401:296–303
55. Farooq U, Zhao YL, Hayat T, Alsaedi A, Liao SJ (2015) Application of the HAM-based Mathematica package BVPh 2.0 on MHD Falkner-Skan flow of nano-fluid. Comput Fluids 111:69–75
56. Mahapatra TR, Gupta A (2002) Heat transfer in stagnation-point flow towards a stretching sheet. Heat Mass Trans 38:517–521
57. Pop S, Grosan T, Pop I (2004) Radiation effects on the flow near the stagnation point of a stretching sheet. Technische Mechanik 25:100–106